Evaluating SWAT model performance, considering different soils data input, to quantify actual and future runoff susceptibility in a highly urbanized basin

Evaluating SWAT model performance, considering different soils data input, to quantify actual and future runoff susceptibility in a highly urbanized basin

Article *in* Journal of Environmental Management · April 2020

DOI: 10.1016/j.jenvman.2020.110625

6 authors, including:


Gianluigi Busico
Aristotle University of Thessaloniki


Nicolò Colombani
Università Politecnica delle Marche


Davide Fronzi
Università Politecnica delle Marche


Marco Pellegrini
LIF srl

Evaluating SWAT model performance, considering different soils data input, to quantify actual and future runoff susceptibility in a highly urbanized basin.

Gianluigi Busico[1], Nicolò Colombani[2,*], Davide Fronzi[2], Marco Pellegrini[3,4], Alberto Tazioli[2], Micol Mastrocicco[1]

[1] DiSTABiF - Department of Environmental, Biological and Pharmaceutical Sciences and Technologies, Campania University "Luigi Vanvitelli", Via Vivaldi 43, 81100 Caserta, Italy;

[2] Università Politecnica delle Marche, Department of Materials, Environmental Sciences and Urban Planning, Via Brecce Bianche 12, 60131 Ancona, Italy

[3] LIF srl, Via di Porto, 159, 50018 Scandicci (FI), Italy

[4] Università Politecnica delle Marche, Department of Agricultural, Food and Environmental Sciences, Via Brecce Bianche 10, 60131 Ancona, Italy

*Corresponding author: Nicolò Colombani: n.colombani@univpm.it

Abstract

The Soil and Water Assessment Tool (SWAT) is a physical model designed to predict the hydrological processes that could characterize natural and anthropized watersheds. The model can be forced using input data of climate prediction models, soil characteristics and land use scenarios to forecast their effect on hydrological processes. In this study, the SWAT model has been applied in the Aspio basin, a small watershed, highly anthropized and characterized by a short runoff generation. Three simulations setup, named SL1, SL2 and SL3, were investigated using different soil resolution to identify the best model performance. An increase of space requirement and calibration time has been registered in conjunction with the increasing soil resolution. Among all simulations, SL1 has been chosen as the best one in describing watershed streamflow, despite it was characterized by the lower soil resolution. A map of susceptibility to runoff for the entire basin was so created reclassifying the runoff amount of four years in five classes of susceptibility, from very low to very high. Eleven sub-basins, coinciding with the main urban settlements, were

identified as highly susceptible to runoff generation. Considering future climate predictions, a slight increase of runoff has been forecasted during summer and autumn. The map of susceptibility successfully identified as highly prone to runoff those sub-basins where extreme flood events were yet recorded in the past, remarking the reliability of the proposed assessment and suggesting that this methodology could represent a useful tool in flood managing plan.

Keywords: Numerical model; hydrogeological risk; runoff; extreme events; risk management.

1 Introduction

Hydrological predictive models (HPM) represent the most recently developed tools in the field of surface water simulation. HPM are currently utilized to assess water and land management strategies in complex watersheds all over the world. In the last century, the need to define water availability and to forecast floods size and duration, together with sediments delivery has become a challenging issue for many local authorities (Wang, 2014). This has come to be very important especially for different life aspects like: i) organization of food supply, ii) security, iii) human health and iv) natural ecosystems. HPM make the users able to manipulate the system's variables/parameters, helping in the understanding of the deep interactions within variables, which are responsible of a system's complexity (Sokolowski and Banks, 2011). The knowledge of this interaction and the availability of quantitative information, that allow the understanding and the description of the hydrological cycle has become mandatory considering the recent interest on climate/land use change's effects (Chaplot, 2005). Starting from the nineteenth century, it is clear how climate variations and variability, together with changes in land use practices, have had a profound impact on basin hydrology, affecting water availability. So, it is crucial to directly quantify the climate change impacts on streamflow at regional and basin scale (Aryal et al., 2018; Bhatta et al., 2019). Sudden changes in the regime of hydro-meteorological events are the main causes of natural extreme events like droughts (Turco et al., 2017), fires (Busico et al., 2019) and floods (Kourgialas and Karatzas, 2011; Shadmehri Toosi et al., 2019) that could affect many regions of the world. Flood events have attracted the global audience and have been recognized as one of the main environmental problems, making the implementation of flood risk scenarios indispensable (Scussolini et al., 2016). Flood events are also highly influenced by the local spatial and temporal characteristics of the area, and small basins can be easily subject to flash food events especially in highly urbanized areas (Tazioli et al., 2015). In this scenario, all the possibilities for flood mitigation need to be integrated into a precautionary and implementation plan. These procedures include the adaptation of land use and infrastructural planning; moreover, especially at the very beginning of flood generation, the knowledge of the runoff generation processes is mandatory to accurately implement the precaution actions (Schüler, 2007). The Soil and Water Assessment Tool (SWAT, Neitsch et al., 2000), was designed to predict the impact of agricultural management practices on water outflow, sediment, nutrient and pesticide loads for large ungauged sub-basins (Arnold et al., 1998). Regarding the hydrological processes, the major ones modelled in SWAT are: i) surface runoff, ii) soil and root zone infiltration, iii) evapotranspiration, iv) soil and snow melting contribution to runoff, and v) baseflow. SWAT has proven to be an efficient tool for simulating many hydrological processes like contaminant transport and soil erosion, and for studying the effects of climate change, land use change and water management practices in different environmental conditions (Ayana et al., 2015; Bhatta et al., 2019; Golmohammadi et al., 2017; Tasdighi et al., 2018). Recently SWAT was also involved in the generation of a flood hazard index (Shadmehri Toosi et al., 2019) using the runoff coefficient. SWAT resulted to be an effective tool for watershed management, while having uncertainties associated with conceptual parameters, physical parameters, drainage area, elevation bands and hydrological response units (HRU) (Shen et al., 2011). Careful calibration, validation and uncertainty analysis are required to achieve the best model performance. Tuo et al. (2016) evaluated SWAT performance using different precipitation input in an Alpine basin. Chaplot (2005) investigated SWAT output changes using different Digital Elevation Models (DEMs) and soil resolutions. More studies, accounting only for the DEM resolution, showed little variation in the yearly calculated runoff (Lin et al., 2013) but substantial changes in the seasonal runoff patterns (Zhang et al., 2014). To date, studies that clearly tackle the role of soil maps resolution are still lacking, except for few examples (Kumar and Merwade, 2009). The aim of this work is to simulate the runoff processes inside a small and highly urbanized basin located near Ancona, central Italy. The Aspio basin is characterized by a Mediterranean climate, with large spatial variability of both rainfall and physical characteristics, which could lead to some difficulties in simulating the runoff regime, respect to other climates (Abdelwahab et al., 2018). The SWAT performance was evaluated using three different soil maps' resolutions, and the best one was chosen to simulate runoff amount for the period 2014-2018. The choice was influenced by several factors like: i) a good fit with real data, ii) the simulation/calibration time needed to obtain reasonable results and iii) the benefit in term of CPU time and field analysis. A total susceptibility map of runoff for the whole basin was also produced accounting for the results of the four simulated years, and it was compared with the observed flooding events. A further evaluation of runoff events for the near future (2040) was also applied, using a downscaled future climate projection of the global climate model (GCM) CNRM-CM6-1 (WorldClim, 2020), to highlight how the predicted changes could positively or negatively affect the runoff phenomena.

2 Material and methods

2.1 Study area

The study area is the Aspio watershed, which belongs to the Marche region (Italy), in the proximity of Ancona city on the Adriatic coast (Figure 1). The Aspio watershed is characterized by the presence of small hills with smoothed shape. The Aspio river springs are located at the confluence of the Offagna, Polverigi and Gallignano ditches, and gather the surface waters of Ancona, Conero Mount and Osimo hills. The Aspio river, the main surface water course of the basin, is a tributary of the Musone river. The geological setting of the Aspio watershed consists of: i) the Meso-Cenozoic limestone sequence, ii) the Mio-Plio-Pleistocene sequence mainly made up of marly clays and marly clays with sandstone layers, and iii) the Quaternary continental deposits made up of silty clay, clayey sand and eluvial-colluvial deposits (Tazioli et al., 2015). Folds with gentle slopes and faults with Apennines and anti-Apennines direction are present in the area. Most of the hills are formed by the Mio-Plio-Pleistocene sequence that gives rise to a peculiar morphology made of gentle ridges and large depressions. The Plio-Pleistocene basin developed along the main tectonic faults and underwent a compressive phase, which was responsible for the final geomorphological evolution of the area (Mirabella et al., 2008). In the Aspio watershed the Quaternary eluvial-colluvial covers are made of sands, silty-sands and clayey silts and can reach a thickness of up to 25 m. The eluvial-colluvial covers host a shallow aquifer that interacts with the Aspio river and its streams throughout the year. The Aspio watershed is characterized by a Mediterranean climate, with an average precipitation of about 800 mm/y in the valleys and 1200 mm/y in mountainous areas (Pellegrini, 2019). The land use is very heterogeneous, according to 2016 Corine Land Cover (CLC) almost 10% of the territory is occupied by urban settlements, equally divided in residential, commercial and industrial units, that are mainly located in the center of the watershed. Agricultural areas area dominated by cereals plantation and occupy more than 60% of the basin, and are directly connected with urban areas. Forests represent less than 2% of the entire watershed.

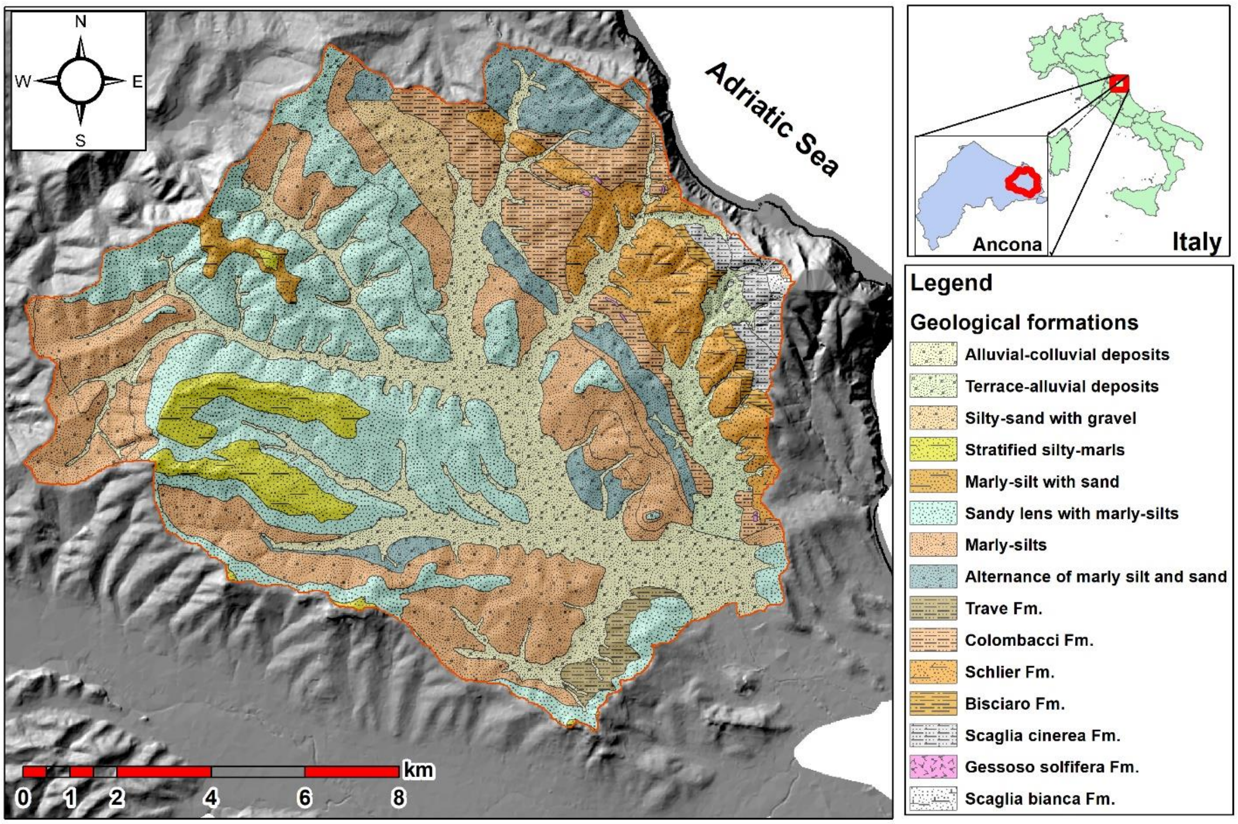

Figure 1: Location and geology of the Aspio Watershed.

Regarding the land use changes inside the Aspio basin, analyzing the land cover maps from the CLC database for the years 2006, 2012 and 2018, no significative changes were recorded trough years. Table S1 shows the different extension of land cover classes based on Level 1 of CLC classification. From 2006 to 2012, very small changes were registered, namely an increase of artificial and forest areas was identified at the expenses of agricultural fields. From 2012 to 2018 instead, no variation has been observed for all the three land-use classes.

2.2 Soil and Water Assessment Tool (SWAT) Model

The Soil and Water Assessment Tool (SWAT) model (Arnold et al., 1998; Arnold et al., 2012) was initially developed by the United States Department of Agriculture (USDA) to simulate the effects of land management practices on the hydrological cycle. SWAT is a physically based and semi-distributed hydrological model able to operate on a different timescale (daily, monthly and annual), generally designed to model and predict continuous long-time runoff, sediment and agricultural chemical yields with watershed and river-basin scale input data. The model is constructed on the concept of hydrologic response units (HRU). A watershed is divided into multiple sub-watersheds, which are further subdivided into HRU, that in turn are portions of a territory characterized by unique land-use/management/soil attributes. The outputs of runoff, sediment, and nutrient loadings from each HRU are generated separately using the input of weather, soil properties, topography, vegetation, and land management practices, and finally summarized to determine the total loadings from each sub-basin. Precisely, SWAT divides the hydrological processes into two different steps: i) land phase, where the input of water, sediment, nutrients and pesticides are calculated in the main channel and inside each sub-basin (Cibin et al., 2010), and ii) a routing phase, that connects all sub-basins by means of the main channel and simulates the movement of water and sediment to the basin outlet. SWAT offers two methodologies for the runoff calculation: i) a modified version of the curve number method (USDA-SCS, 1972) and ii) the Green–Ampt infiltration method, while the Modified Universal Soil Loss Equation (MUSLE) (Williams, 1995) is applied to predict sediment generation.

2.3 Model set-up

The SWAT model for the Aspio basin has been built using information concerning morphology, land cover, soil properties and climate data. The ArcSWAT 2012 version on ArcGIS 10.2 platform has been used for the elaboration in this work. In Table S2 all the sources of the utilized data are listed. For the realization of a regular SWAT simulation three main steps are needed. First, using the "Watershed automatic delimitation" all the topographical inputs were calculated starting from a 20 m resolution Digital Elevation Model (DEM) to define the watershed features like boundaries, river network, sub-basins, and to derive slope-related parameters. For the Aspio basin, an area of 155 km^2 has been divided in 33 sub-basins (Figure 2) with a minimum and maximum elevation of 8 m and 540 m above sea level (a.s.l.), respectively. The second phase includes the HRU definition, intersecting data of slope, land cover and soil property information. The slope ranges were established using the 20 m resolution DEM and classified in 3 classes: less than 5°, between 5° and

15°, and more than 15°. As no significative changes in land use were recorded in the last 20 years, the CLC map for 2018 has been used for HRU delimitation. Eleven land covers were identified (mainly industrial, residential, agricultural and agro-forestry) and homogenized with SWAT2012 crop's default database. Regarding soils' properties, SWAT requires the information about soil hydraulic conductivity (Ks), soil water content, texture, percentage of organic carbon, soil albedo ad more. For this study three different soil maps have been used (Figure S1), inasmuch, the soil properties represent one of the three information needed in the construction of the HRU. The first simulation (SL1) utilized the soil information derived from the Digital Soil World Map (DSMW; FAO, 2007) with a scale of 1:5 million. According to FAO DSMW classification (Figure S1a), the Aspio basin is characterized by one soil category (Eutric Gleysol) with a Ks of 7.32 mm/h, a soil bulk density (BD) of 1.3 g/cm^3 and an available water capacity (AWC) of 0.164 mm H_2O/mm of soil. For the second simulation (SL2) a more detailed soil map was constructed based on the geologic characteristics of the study area with a scale of 1:10000. In this case the classification was done using at least 3 Ks values of the topsoils (Figure S1b) measured with a double ring infiltrometer in the respective geological formations, while all the other parameters have been integrated using the SWAT soil's default database selecting the soil type and texture. Thirteen soil formations (Figure S1c) were identified with a Ks ranging from 0.35 to 324 mm/h, an average BD of 1.5 g/cm^3 and AWC values from 0.073 to 0.175. The last simulation (SL3) was constructed using only those soil units (Figure S1b) with the maximum extension among the thirteen previously utilized for SL2. In this case three main soil units have been chosen as representative of the entire basin. Soil data for SL2 and SL3 come from previous analyses realized by Università Politecnica delle Marche (Mattioli, 2012) and are shown in Table S3 together with soil data for SL1. Parameters like Ks, clay, silt and sand content have been measured in the field while the values of AWC and BD were adjusted using a hydraulic property calculator and integrated with the default SWAT2012 input database's values. For all the three simulation 33 sub-basins were created and further divided into HRU, using a threshold of less than 10% for land use, for soil type, and slope. The HRU threshold was employed to further discretize each sub-basin, especially for SL2 and SL3 where a great heterogeneity in land use, soil and slope was found (Her et al., 2015). The last necessary input are the meteorological data. SWAT asks for daily variables of precipitation, temperature, relative humidity, solar energy, and wind speed. Among these parameters, precipitation is directly involved in the runoff calculation, and together with temperatures, wind speed, humidity and solar radiation, is utilized for the calculation of the evapotranspiration. Depending to the data availability three methodology are provided for the calculation of potential evapotranspiration (Aschonitis et al., 2017): i) Priestly-Taylor, ii) Penman/Monteith and iii) Hargreaves. The software also offers a weather generator tool to fill missing data for certain periods and furthermore it allows for the simulation of all climate variables, if an historical database related to the watershed is available. In this case the Hargreaves method has been adopted for the estimation of the evapotranspiration rates on the catchment for all the three simulations, instead of using the weather simulation tool according to available climate data. Daily precipitation together with maximum and minimum temperature data, coming from four meteorological stations (Osimo, Ancona, Baraccola, Svarchi) located inside the Aspio basin, have been used for the simulations. Such data are part of Marche Region Meteorological-Hydrological Information System (SIRMIP, 2020). To examine the future trend of runoff generation the values of predicted temperatures and precipitations coming from the WorldClim database for the period 2021–2040 have been utilized for a post validation SWAT run. The selected database for the period 2021–2040 is a Coupled Model Intercomparison Project (CMIP6) downscaled future climate projection of the global climate model (GCM) CNRM-CM6-1 with the Shared Socio-economic Pathway (SSP) 2-4,5, at a spatial resolution of 2.5 minutes (WorldClim, 2020). Generally for Mediterranean area an average increase of 1.5–2.0° C of temperature is predicted, especially in the summer period (Giorgi and Lionello, 2008) together with a decrease of precipitation with a marked seasonal regime: a decrease of around 30-40 % in precipitation during the summer period and an increase of 25-20% during the winter period (Bucchignani et al., 2016; Mastrocicco et al., 2019). Also, in this case the Hargreaves method has been applied for PET calculation accordingly to data availability.

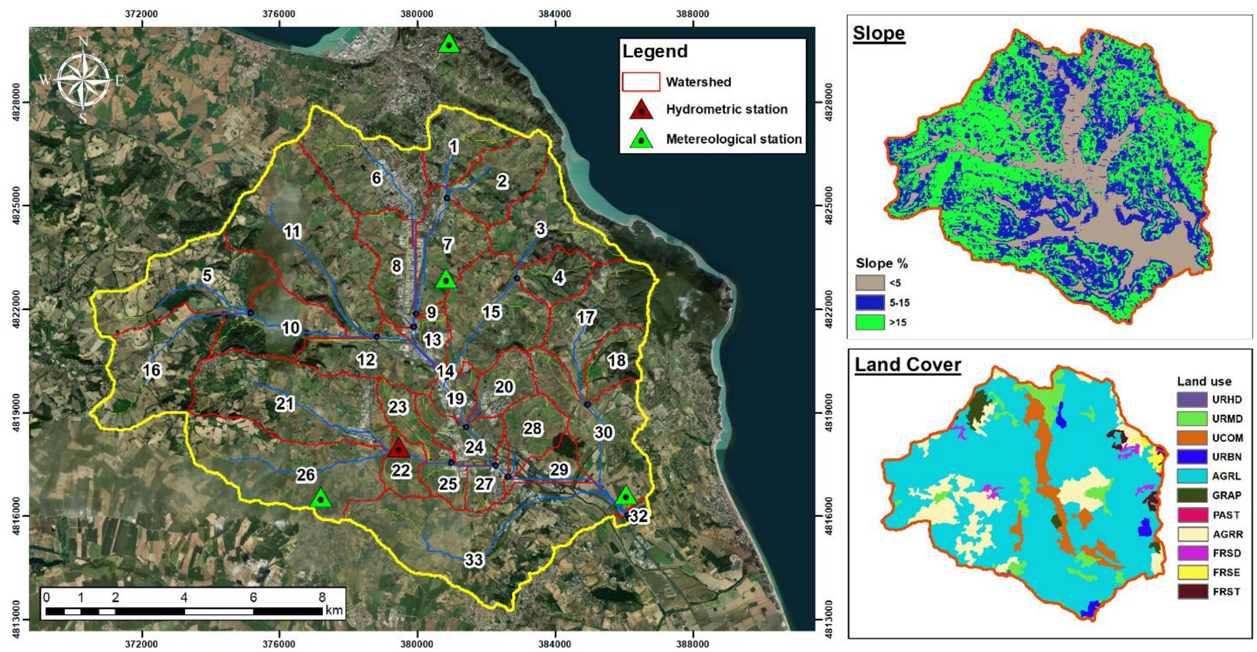

Figure 2: SWAT model setup for the Aspio basin containing watershed subdivision, slope classes and land use dominance.

2.4 Calibration and validation

The main requirements for a model evaluation are: i) measuring the reliability of the criteria and ii) the robustness of the methodology. This is investigated through a calibration and validation procedure. The auto-calibration tool was used as calibration and validation technique, via the standalone program SWAT-CUP using the Sequential Uncertainty Fitting version 2 (SUFI-2) algorithm (Abbaspour, 2015). SUFI-2 is well known to estimate both parameters and model uncertainties in hydrological models (Abbaspour, 2015). Within SWAT-CUP the user can select the most sensitive parameters that could influence the observed outputs (e.g. streamflow, sediment/chemical yield) and choose a range of variation (e.g. ±25% of the initial value). During the calibration procedure the algorithm tries different combination of parameters within their new ranges and calculates the effect on the fitting between observed and simulated variables. Finally, the results obtained from the calibration\validation procedure are evaluated computing different statistical indices. In the present study the robustness of the applied methodology was defined by means of three indices: coefficient of determination (R^2), Nash-Sutcliffe efficiency (NSE) and percent of bias (PBIAS). The indices are calculated following the formulas below:

$$R^2 = \left(\frac{\sum_{i=1}^{n} (K_{predicted} - \bar{K}_{predicted})(K_{measured} - \bar{K}_{measured})}{\sqrt{\sum_{i=1}^{n} (K_{predicted} - \bar{K}_{predeicted}) * \sum_{i=1}^{n} (K_{measured} - \bar{K}_{measured})}} \right)^2 \quad (1)$$

$$NSE = 1 - \frac{\sum_{i=1}^{n} (K_{predicted} - K_{measured})^2}{\sum_{i=1}^{n} (K_{predicted} - \bar{K}_{predicted})^2} \quad (2)$$

$$PBIAS = \left(\frac{\sum_{i=1}^{n} (K_{measured} - K_{predicted})}{\sum_{i=1}^{n} K_{predicted}} \right) * 100 \quad (3)$$

where $K_{predicted}$ is the value predicted from the model, $\bar{K}_{predicted}$ is the average value between the predicted values. $K_{measured}$ is the value measured in field and $\bar{K}_{measured}$ is the average value between the real data.

According to Moriasi et al. (2007), the optimal thresholds for the three statistical indices for an acceptable streamflow simulation are $R^2 \geq 0.50$, NSE ≥ 0.50 and PBIAS ± 25%.

Simulations have been calibrated and validated using daily streamflow data coming from the Scaricalasino hydrometric station (Figure 2) for the period 2015-2018. Real data were compared with the streamflow outlet of sub-basin 24. Calibration was performed using daily data for the period 2015-2016 and validation was performed for the period 2017-2018.

3 Results and Discussion

One of the first result identified, comparing the HRU formation for SL1, SL2 and SL3 was the increase in complexity of the model together with a rise of computational resources needed in terms of Gigabyte occupied. While SL1 recognized 351 HRU, SL2 and SL3 identified 683 and 1029 HRU, respectively. It is clear how the different spatial discretization of soil types for the three simulations directly influenced the number of HRU together with model weight and complexity. After the set-up procedure, all the three models were run for the period 2010-2018 using the first four years as warm-up period.

3.1 Sensitivity analysis and model performance evaluation

As described in paragraph 2.4, the SWAT-CUP program with SUFI-2 algorithm has been used for the calibration/validation procure of SL1, SL2 and SL3. The calibration parameters have been chosen trough literature review. According to Malagò et al. (2015), Khelifa et al. (2017) and Chen et al. (2019) eleven parameters (Table 1) were identified as the most relevant in affecting the stream-flow simulation. The NSE index was chosen as optimization function for the calibration procedure and, together with PBIAS and R^2, it was used in this study to check model performance, following the boundary value suggested by Moriasi et al. (2007). The calibration procedure was carried out for SL1, SL2 and SL3 retaining the same initial parameters setup. A total of 2000 runs of calibration, divided in four interactions of 500 runs each, were performed for each simulation. The first interaction was done using the initial boundary (Min and Max columns in Table 1) of the chosen eleven parameters as suggested by Abbaspour (2015). The increasing number of HRU from SL1 to SL3 and SL2, together with the model complexity, was accompanied by a general increase of time needed for successfully run a calibration procedure.

Table 1: List of parameters used for model calibration.

Parameter Name	Description	Method	Min Value	Max Value
CH_N2.rte	Main channel Manning number	Replace	0	0.3
CH_K2.rte	Effective hydraulic conductivity	Replace	5	130
ALPHA_BF.gw	Baseflow alpha factor	Replace	0	1
SOL_AWC.sol	Available water capacity of the soil	Relative	-0.2	0.4
ESCO.hru	Soil evaporation compensation factor	Replace	0.8	1
SOL_BD.sol	Moist Bulk density	Relative	-0.5	0.6
GW_REVAP.gw	Groundwater evaporation coefficient	Replace	0	0.2
ALPHA_BNK.rte	Baseflow alpha factor for bank storage	Replace	0	1
SOL_K.sol	Saturated hydraulic conductivity	Relative	-0.8	0.8
GW_DELAY.gw	Groundwater delay time	Replace	30	450
CN2.rte	Initial SCS curve number	Relative	0	0.3

According to Rouholahnejad et al. (2012) the processing time of these models can be rather long, not allowing proper model calibration and uncertainty analysis. For SL1, SL2, and SL3, maintaining the same number of parameters to be calibrated, an increase in time was recorded with increasing number of HRU. For 100 simulations of SUFI-2 performed on a commercial 3.60 GHz CPU with 12 GB RAM, SL1, SL2 and SL3 took 1 hour, 2 hours and 30 minutes, and 1 hour and 55 minutes processing time, respectively. SWAT-CUP allows to perform a local or a global sensitivity analysis: i) the local sensitivity demonstrates the sensitivity of a single variable to the changes if all other parameters values are kept constant, while ii) the global sensitivity analysis explores all the possible input combination between parameters. So, the utilization of the global sensitivity promotes a multilinear regression of the entire input space, giving an estimation of the overall effect of all the inputs or their combined effect on the variation of output based on many models runs (Song et al., 2015). In this work the global sensitivity analysis has been applied as it was found to be the most recommended for hydrogeological processes from many authors (Baroni and Tarantola, 2014; Rosolem et al., 2012) The results of the sensitivity analysis for SL1, SL2 and SL3 are shown in Table 2.

Table 2: Sensitivity analysis results and calibrated values for SL1, SL2, and SL3. For parameters description please refer to Table 1. Values in bold are the most sensitive parameters.

SENSITIVITY Parameter Name	SL1 P-Value	SL2 P-Value	SL3 P-Value	SL1 Calibrated value	SL2 Calibrated value	SL3 Calibrated value
CN2.rte	**0.00**	**0.00**	**0.00**	-0.35	-0.41	-0.35
CH_K2.rte	**0.00**	**0.00**	**0.00**	21.2	26.50	27.50
ALPHA_BF.gw	**0.00**	**0.28**	**0.00**	0.00	0.05	0.00
SOL_AWC.sol	**0.00**	0.65	**0.00**	0.14	0.00	0.25
ESCO.hru	**0.01**	0.68	**0.00**	0.82	0.84	0.84
SOL_BD.sol	**0.02**	**0.16**	**0.03**	-0.41	-0.25	-0.36
GW_REVAP.gw	**0.28**	**0.24**	0.80	0.14	0.15	0.14
ALPHA_BNK.rte	**0.43**	0.92	**0.30**	0.06	0.00	0.05
SOL_K.sol	0.65	**0.01**	**0.04**	-0.28	-0.28	-0.45
GW_DELAY.gw	0.88	**0.28**	0.90	222	200.0	255.0
CH_N2.rte	0.98	**0.17**	0.93	0.15	0.13	0.17

Among the eleven chosen parameters, eight sensitive ones have been detected to be important in regulating the streamflow generation for all the simulations (bold values in Table 2). Each simulation differs for the type of sensitive parameter and for its relative weight: i) for SL1, SCS runoff curve (CN2) and effective hydraulic conductivity for the main channel (CH_K2) together with some soil characteristics like soil water content (SOL_AWC), bulk density (SOL_BD), soil evaporation factor and baseflow factor (ALPHA_BF) were identified as the factors that produced the higher impact on streamflow simulation, ii) in SL2, besides CH_N2, CH_K2 and ALPHA_BF also soil hydraulic conductivity (SOL_K), groundwater delay time (GW_DELAY), and Manning's value (CH_N2) were detected as sensitive parameters, and iii) for SL3 the result is almost the same as for SL1, with the only introduction of SOL_K. These results indicate that the greater number of soil units are considered, the more importance is gained by the hydraulic conductivity (SOL_K) in the streamflow/runoff generation. So, after the first interaction, the following ones were started using only the eight sensitive factors for SL1, SL2 and SL3 to obtain the fitted parameters' values (Table 2). The final calibration performances of the three models (SL1, SL2 and SL3) were assessed using three statistical indices and are reported in Table 3.

Table 3: Performance analysis of the SWAT model in simulating streamflow during the calibration procedure. Values in bold are above the optimal thresholds defined by Moriasi et al. (2007).

Statistical parameters	Moriasi et al. (2007)	SL1	SL2	SL3
Coefficient of determination (R^2)	**≥0.50**	**0.76**	**0.65**	**0.71**
Nash-Sutcliffe efficiency (NSE)	**≥0.50**	**0.65**	0.36	0.42
Percent bias in volume (PBIAS)	**±25**	**6.1**	-56.1	-32.9
CPU time for 100 runs (minute)		**60 min**	150 min	115 min

As shown in Table 3, SL1 is the only one whose values are within the range of acceptability for the three statistical indicators. SL1 shows a high R^2 of 0.76 and a good NS value of 0.65, nevertheless, the positive value of PBIAS (6.1%) indicates a little underestimation of the daily streamflow. Regarding SL2 and SL3, two of the three statistical indices (NSE and PBIAS) are outside the range qualifying an acceptable performance and moreover, both SL2 and SL3 greatly overestimate the streamflow (negative PBIAS). Figure 3 shows a comparison of the three model simulations with real data using monthly values. Among the models, SL1 shows a good monthly correspondence with real data and a comparable general trend. On the other hand, SL2 and SL3 while showing a good general trend, overestimate the streamflow values 3 to 4 times. The Figure S2, S3 and S4 represent the main water balance components for the three simulations. The main difference concerns the evapotranspiration that is maximal in SL1 and is reduced in the other two scenarios. The recharge to the shallow aquifer slightly reduces in SL2 and SL3 compared to SL1, while the lateral flow in SL2 and SL3 increases, and the runoff for SL2 and SL3 is three time higher (150 mm) than SL1 (41 mm). In general, in SL2 (264 mm) and SL3 (255 mm) a higher amount of water returns to the streams (runoff, later flow and return flow) respect to SL1 (148 mm) explaining the streamflow overestimation shown in Figure 3. Moreover, ordering the simulations according to the number of soil units employed, a general linear decrease of the statistical indices from SL1 (one soil) to SL3 (three soils) and finally to SL2 (thirteen soils) is recorded. This finding agrees with Chaplot (2005), which stated that not always the extra cost and labor to obtain the greatest precision in input, like soil characteristics, bring to more accurate predictions. So, considering that SL2 and SL3 despite involving more detailed information have showed the worse simulation results, SL1 has been chosen as reference simulation for the validation procedure. It is also true that SL2 and SL3 showed a good R^2 with real data, following the same trend, but with higher predicted volume. It is surely possible that with further modifications of some soil parameters, together with more calibration runs, those simulations could bring to better results but, at the same time, this could be highly time consuming and not cost effective. So, there are several main reasons why the SL1 has been chosen: i) open access database has been used (no field analysis needed), ii) less space requirement and iii) an acceptable simulation time to achieve satisfactory results. The model's performance for the calibration and validation periods are represented in Figure 4. Both calibration and validation are satisfactory with NSE and $R^2 \geq 0.50$ and PBIAS ± 25%. For the validation procedure all the three statistical indices are in the range of a "good" calibration with a R^2 of 0.80, an NSE of 0.60 and a PBIAS of -15.35%. The streamflow representation in Figure 4 confirms a little underestimation for the calibration (positive PBIAS) and an overestimation for the validation procedure (negative PBIAS), but in any case within the acceptable range (PBIAS ±25%). In general, SL1 shows a satisfactory model performance especially in simulating the highest peaks of streamflow.

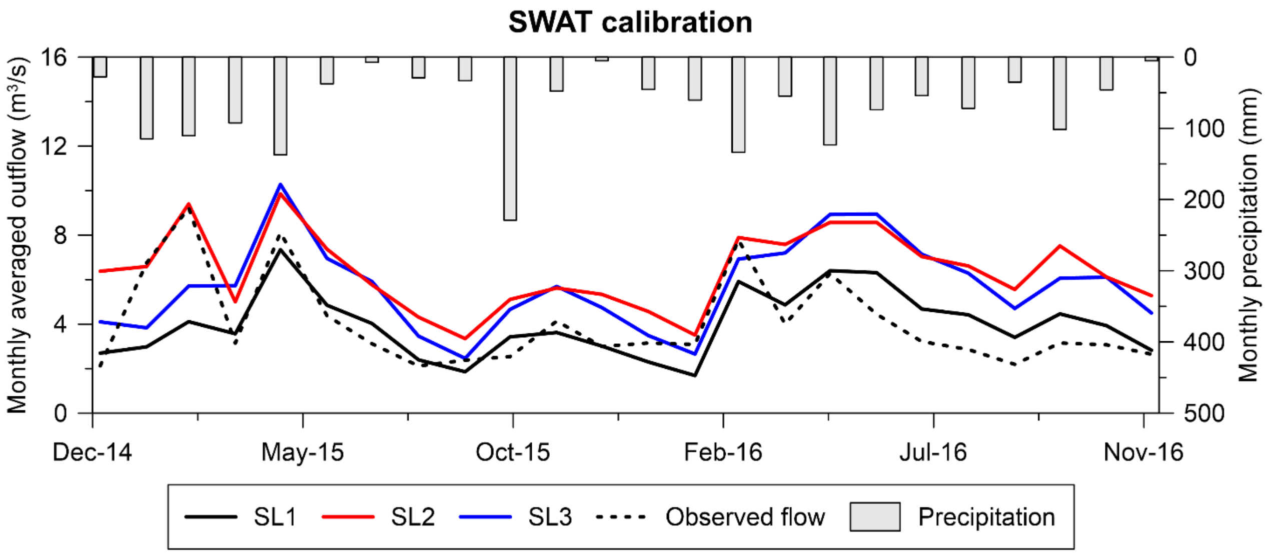

Figure 3: SWAT streamflow simulation for SL1, SL2 and SL3 after calibration procedure.

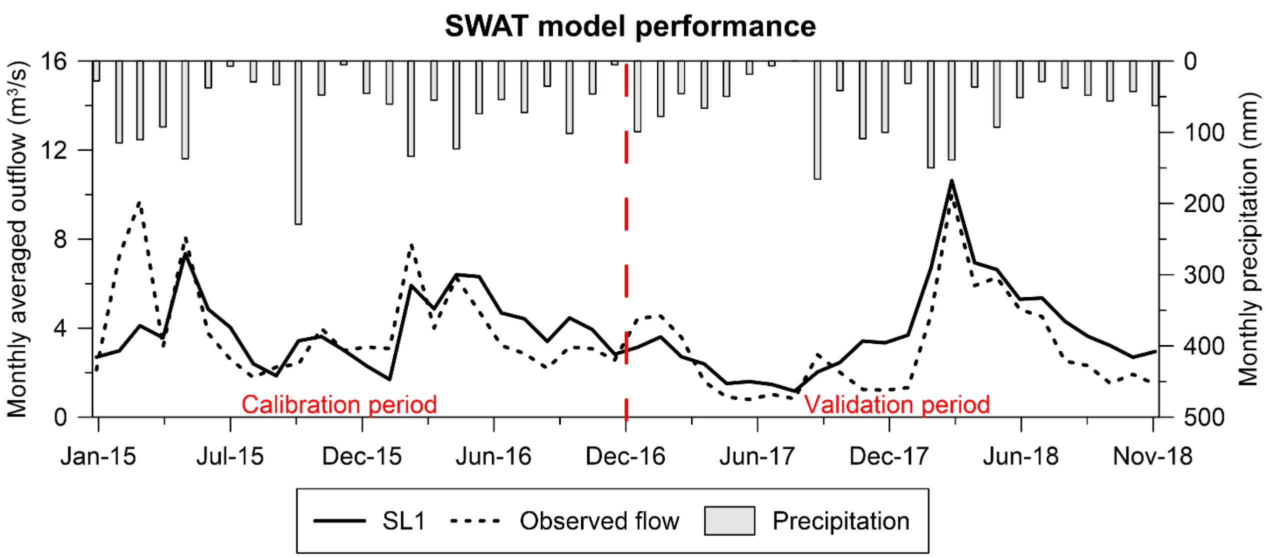

Figure 4: SWAT calibration/validation for SL1.

3.3 SWAT runoff generation areas and total runoff susceptibility

Following the calibration/validation procedure, the SWAT model was run for the period 2015-2018 in the entire basin. Among the available model's outputs, it was chosen to integrate the SWAT output SURQ (Surface runoff contribution to streamflow during time step, mm H_2O) for the 4 years of simulation. This choice depends to some characteristics of the study area where a short runoff time occurs, that can lead to high flood risks especially in small basin (Pappenberger et al., 2005). The runoff values for the 33 sub-basins range between a minimum of 3 mm/y to over 250 mm/y in the 4 simulated years. Figure 5 shows a spatial representation of runoff amounts for the Aspio basin in the analyzed period. The values of runoff were here reclassified in 5 qualitative classes from very low to very high using the geometrical interval, that is the most used classification interval for the spatial representation of many environmental parameters (Barzegar et al., 2019; Huan et al., 2012; Kazakis et al., 2019). Looking at the maps (Figure 5) it is possible to appreciate how, despite the change in meteorological condition within the analyzed years, some sub-basins seem to be always characterized by higher amount of runoff compared to others. The sub-basins 1, 6, 7, 8, 12, 13, 19, 20, 24, 27 and 28 are always characterized by high and very high amount of runoff. In particular, sub-basin 24 generates less runoff for 2015 and 2017 respect to 2016 and 2018. In these two latter years, even thou cumulative precipitation was smaller compared to 2015 and 2017, extreme rain fall events have been registered which lead to an increase in the annual runoff value. Considering the four simulated years, a total susceptibility map to runoff events has been produced. This map allows to identify the area that, independently from meteorological condition, could generate high amount of runoff. To realize the final map, each one of the yearly maps have been reclassified from 1 (very low) to 5 (very high) according to runoff values. Finally, a linear combination of the yearly map divided for the number of years involved has been produced using the raster calculator tool in ArcGIS 10.2. The total susceptibility map to runoff production is shown in Figure 6. The sub-basins characterized by higher runoff rate remained the same previously mentioned and are mainly concentrated in the center of the basin, while the ones with lower production of runoff spread to the East and West boundaries. The classification follows the spatial heterogeneity of land-use. The map shows how the areas susceptible to generate high runoff amount follow the distribution of the urban/commercial areas, while the agricultural and forested areas, despite the higher slope, generate less runoff. The susceptibility of urban areas to runoff is generally higher than agricultural and forestry ones (Ferreira et al., 2012, 2015). In this situation, the runoff could be up to 5 times higher in a developed urban area compared to a forestry territory where it is reduced by evapotranspiration and infiltration. The same happens also if the agricultural landscape is developed into an urban area, here, the runoff tends to increase even more due to an increasing imperviousness of the surface (Branger et al., 2013; Dietz and Clausen, 2008).

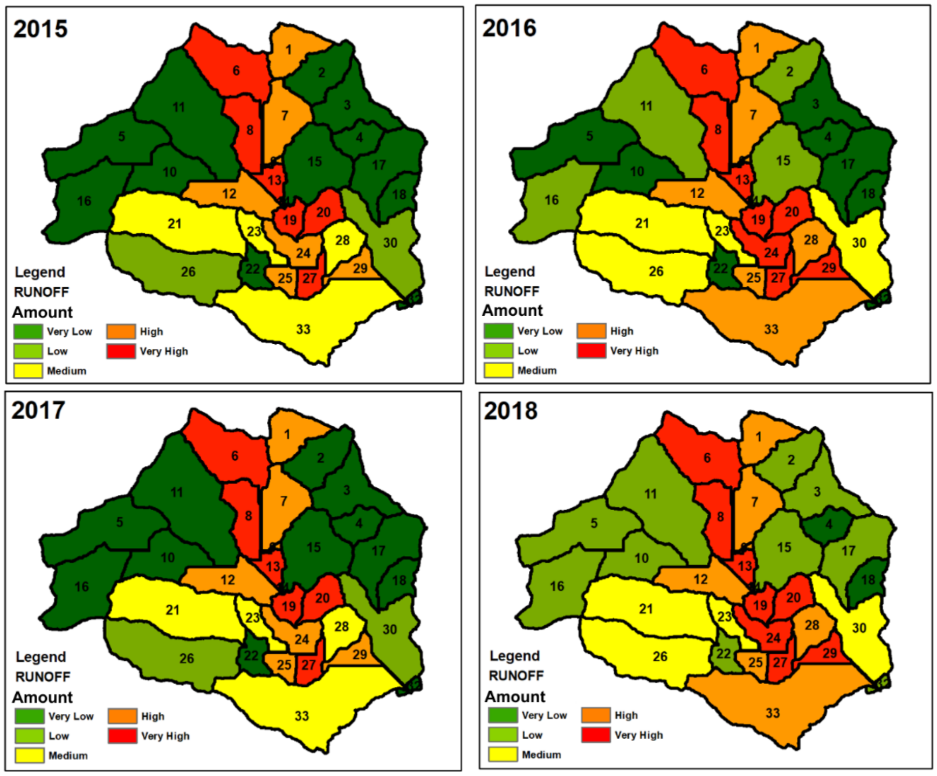

Figure 5: Qualitative representation of the runoff amounts for the four simulated years.

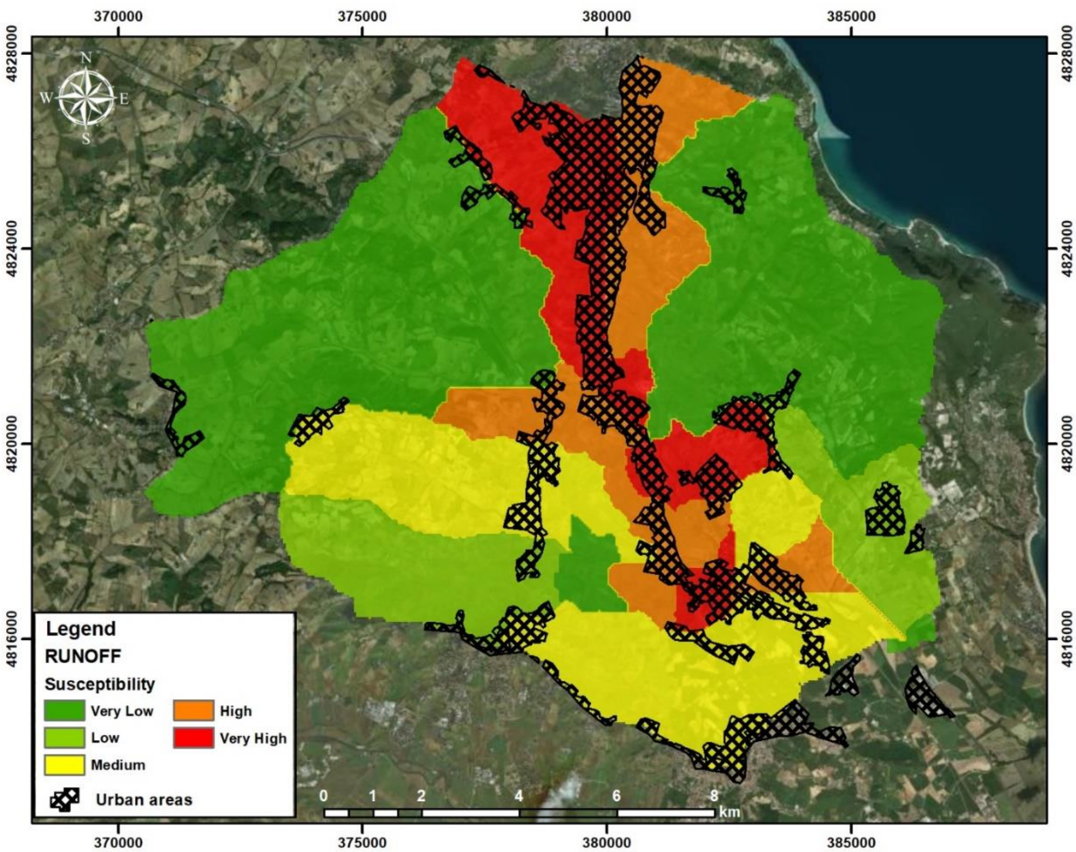

Figure 6: Total runoff susceptibility map for the Aspio basin.

Another concern for the urban area is represented by the manmade drainage system that becomes the only way of discharge. Despite of the naturally meandering streams and rivers, channels are normally straight, and the resistance of concrete channels is normally lower than that of natural streams and rivers. These could bring to shorten the runoff time and increase the peak flow downstream (Bedient et al., 2012) with a consequently higher flood risk. To account for the possible runoff changes due to land use variations, a series of model scenarios were produced using different CLC (2006, 2012, 2018) without any significant change. Even producing a piecewise SWAT simulation using CLC 2006 for the years from 2010 to 2012, CLC 2012 from 2012 to 2018 and CLC 2018 for 2018, no changes in the runoff outputs were detected. This confirms that inside a basin where no significative changes in land use occur, the low and high peaks of runoff trough years are entirely dependent on climate variability. While, if land use changes are large (e.g. >40%) during the simulated period, calculated monthly and daily runoff can considerably be affected (Lin et al., 2015). Following this assumption, a further runoff prediction considering world climate prediction under SSP2-4.5 scenario is shown. In this case the daily precipitation and temperature for all the four meteorological stations were modified considering the SSP2-4.5 scenario prediction, while maintaining unchanged the land use distribution. For the precipitations pattern, an overall 20% of decrease is predicted for 2040, but the decrease will not be regularly distributed during the year. The decreasing trend is also confirmed from a regional study on historical climate data, together with an increase of extreme events like storms and droughts, which can further promote the occurrence of calamitous events (Gentilucci et al., 2020). Thus, a decrease of 35% in precipitation has been applied to the months of January, February and March; while a decrease of 20% has been applied to May, November and December and an increase of 25% to June, July, August and September. The months of April and October have not undergone any change. The decrease/increase rate has been decided considering the average monthly precipitation values for the period 2020-2040 using the CNRM-CM6-1 Earth system model provided in Figure S5. Using the same approach an average of 1.5° C has been added to minimum and maximum temperatures for evapotranspiration calculation. Considering these changes, a new SWAT run was applied for the period 2036-2040 using the same calibrated values of SL1. Runoff for sub-basin 24 has been chosen for runoff comparison since it belongs to a high runoff susceptibility class. Figure 7 shows the comparison of runoff for a period of two years, 2017-2018 for the actual situation and 2039-2040 for the future. Comparing the predicted data of runoff simulated by SWAT, a general increase has been predicted for the years 2039-2040, despite the annual precipitation decrease. The runoff switches from 199 mm in 2017-2018 to 245 mm in 2039-2040. Looking at Figure 7, the same amount of runoff is recorded in winter and spring (December, January, February, March and April) and a slight increase during summer (especially for May, June and July). This finding suggests that even those months which are generally considered safe have become critical, since the more abundant precipitation in such months, together with the increase of the extreme events, could increase the susceptibility to extreme flood events.

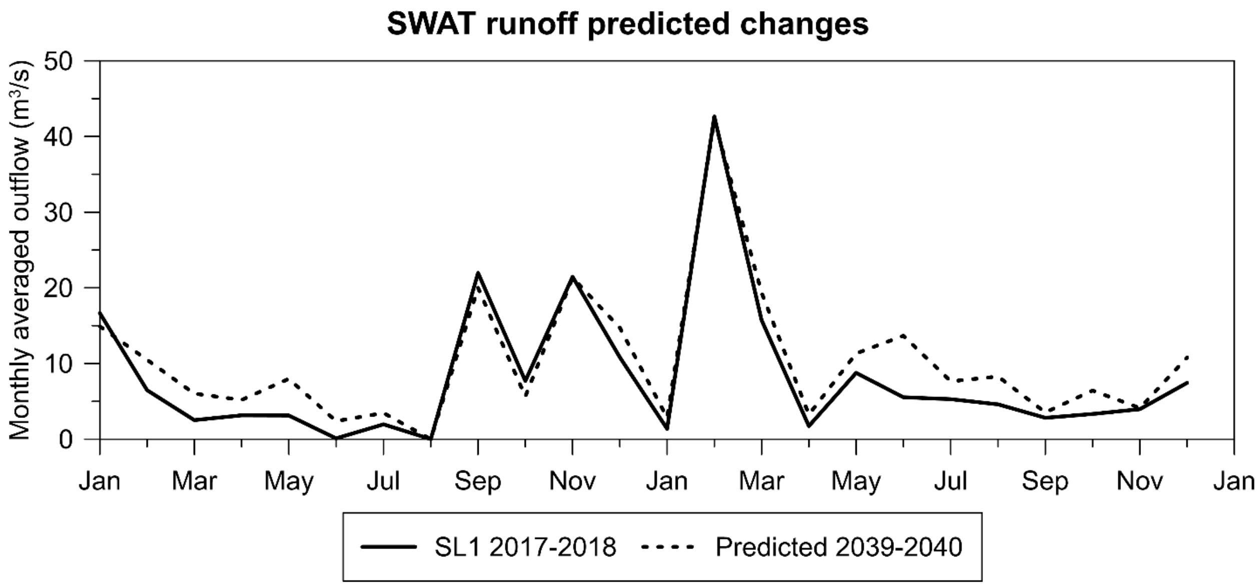

Figure 7: Comparison of the monthly runoff calculated (2017-2018) and predicted (2039-2040) for sub-basin 24 for the SL1.

Finally, the analysis of the Civil Protection report on the flooding event occurred on the 16th of September 2006 (Civil Protection Marche Region, 2006) highlighted that the urban areas flooded during that extreme event (Figure S6), located between Aspio Terme and Osimo Stazione villages, are estimated as high and very high zones of runoff susceptibility in the total runoff susceptibility map for the Aspio basin shown in Figure 6. Moreover, a second and less important flooding event was recorded between the 9th and 10th of March 2010 (Civil Protection Marche Region, 2010) where numerous distributed inundations occurred within the lower portion of the Aspio basin, in coincidence with the high and very high zones of runoff susceptibility. This further contributes to confirm the reliability of the applied methodology, making it a useful tool for local authorities in preventing flood events inside urban areas.

4 Conclusions

SWAT model performance in simulating the hydrogeological regime has been evaluated for the Aspio basin, near Ancona city (Italy) using different soil configurations. Three soil maps were employed: i) FAO DWSM, ii) soil information derived from local geology, and iii) a soil map obtained considering only the three main units (higher extension) identified from local geology. The results of the calibration procedure indicate a worsening of the performance if an increasing number of soil units is considered. Within the three simulations, only SL1 showed a good performance and was so further utilized in the validation procedure. The final statistical indices for SL1 confirmed that this simulation is the best one for the simulation of the daily streamflow for the Aspio basin. Furthermore, the model's output of yearly runoff was integrated for 2015, 2016, 2017 and 2018. The produced map shows that some sub-basins are always characterized by a high amount of runoff. The runoff susceptibility map, realized considering the four yearly maps indicates the same sub-basins as high susceptible to runoff. Inside these areas, characterized by high urbanization, short runoff times could occur, increasing the peak flow downstream and consequently the flood risk. This elaboration represents a valuable tool for managing implementation plans and preventive targeted actions for those areas more susceptible to runoff generation. The general approach here employed can be adopted in many other small watersheds characterized by Mediterranean climate and highly anthropized.

5 References

Abbaspour, K.C., 2015. Calibration and Uncertainty Programs. SWAT-Cup User Manual.

Abdelwahab, O.M.M., Ricci, G.F., De Girolamo, A.M., Gentile, F., 2018. Modelling soil erosion in a Mediterranean watershed: Comparison between SWAT and AnnAGNPS models. Environ. Res., 166, 363-376. http://doi.org/10.1016/j.envres.2018.06.029

Arnold, J.G., Moriasi, D.N., Gassman, P.W., Abbaspour, K.C., White, M.J., Srinivasan, R., Santhi, C., Harmel, R.D., Griensven, A., Van-Liew, M.W., Van Kannan, N., Jha, M.K., 2012. SWAT: model use, calibration, and validation. 2012 American Society of Agricultural and Biological Engineers ISSN 2151-003255: 1491–1508.

Arnold, J.G., Srinivasan, R., Muttiah, R.S., Williams, J.R., 1998. Large-area hydrologic modeling and assessment: Part I. Model development. J. Am. Water Resour. As. 34, 73–89. https://doi.org/10.1111/j.1752-1688.1998.tb05961.x

Aryal, A., Shrestha, S., Babel, M.S., 2018. Quantifying the sources of uncertainty in an ensemble of hydrological climate-impact projections. Theor. Appl. Climatol. 1-17 (2359-3). https://doi.org/10.1007/s00704-017-2359-3

Aschonitis, V.G., Papamichail, D., Demertzi, K., Colombani, N., Mastrocicco, M., Ghirardini, A., Castaldelli, G., Fano, E.A., 2017. High-resolution global grids of revised Priestley–Taylor and Hargreaves–Samani coefficients for assessing ASCE-standardized reference crop evapotranspiration and solar radiation. Earth Syst. Sci. Data, 9, 615–638. https://doi.org/10.5194/essd-9-615-2017

Ayana, E.K., Worqlul, A.W., Steenhuis, T.S., 2015. Evaluation of stream water quality data generated from MODIS images in modeling total suspended solid emission to a freshwater lake. Sci. Total Environ. 523, 170–177. http://doi.org/10.1016/j.scitotenv.2015.03.132

Baroni, G., Tarantola, S., 2014. A general probabilistic framework for uncertainty and global sensitivity analysis of deterministic models: a hydrological case study. Environ. Modell. Softw. 51, 26–34. http://dx.doi.org/10.1016/j.envsoft.2013.09.02

Barzegar, R., Asghari Moghaddam, A., Adamowski, J., Hossein Nazemi, A., 2019. Delimitation of groundwater zones under contamination risk using a bagged ensemble of optimized DRASTIC frameworks. Environ. Sci. Pollut. Res. 26 (8), 8325-8339 https://doi.org/10.1007/s11356-019-04252-9

Bedient, P.B., Huber, W.C., Vieux, B.E., 2012. Hydrology and Floodplain Analysis: Fifth Edition. Harlow: Pearson

Bhatta, B., Shrestha, S., Shrestha, P.K., Talchabhadel, R., 2019. Evaluation and application of a SWAT model to assess the climate change impact on the hydrology of the Himalayan river basin. Catena, 181. http://doi.org/10.1016/j.catena.2019.104082

Branger, F., Kermadi, S., Jacqueminet, C., Michel, K., Labbas, M., Krause, P., Kralischd, S., Braud, I., 2013. Assessment of the influence of land use data on the water balance components of a periurban catchment using a distributed modelling approach. J. Hydrol. 505, 312–325. https://doi.org/10.1016/j.jhydrol.2013.09.055

Bucchignani, E., Montesarchio, M., Zollo, A.L., Mercogliano, P., 2016. High-resolution climate simulations with COSMO-CLM over italy: Performance evaluation and climate projections for the 21st century. Int. J. Climatol. 36(2), 735-756. http://doi.org/10.1002/joc.4379

Busico, G., Giuditta, E., Kazakis, N., Colombani, N., 2019. A Hybrid GIS and AHP Approach for Modelling Actual and Future Forest Fire Risk Under Climate Change Accounting Water Resources Attenuation Role. Sustainability. 2019 (11), 7166. https://doi.org/10.3390/su11247166

Chaplot, V., 2005. Impact of DEM mesh size and soil map scale on SWAT runoff, sediment, and NO3-N loads predictions. J. Hydrol. 312(1-4), 207-222. http://doi.org/10.1016/j.jhydrol.2005.02.017

Chen, Y., Xu, C.-Y., Chen, X., Xu, Y., Yin, Y., Gao, L., Liu, M., 2019. Uncertainty in simulation of land-use change impacts on catchment runoff with multi-timescales based on the comparison of the HSPF and SWAT models. J. Hydrol. 573, 486-500. http://doi.org/10.1016/j.jhydrol.2019.03.091

Cibin, R., Sudheer, K., Chaubey, I., 2010. Sensitivity and identifiability of stream flow generation parameters of the SWAT model. Hydrol. Process. 24 (9), 1133–1148. https://doi.org/10.1002/hyp.7568

Civil Protection Marche Region, 2006. Available online at: http://www.regione.marche.it/Portals/0/Protezione_Civile/Manuali%20e%20Studi/Rapporto_Evento_2006_09_16.pdf?ver=2016-04-19-125842-000

Civil Protection Marche Region, 2010. Available online at: http://www.regione.marche.it/Portals/0/Protezione_Civile/Manuali%20e%20Studi/Rapporto_Evento_2010_03_09.pdf?ver=2016-04-19-125218-000

Dietz, M.E., Clausen, J.C., 2008. Stormwater runoff and export changes with development in a traditional and low impact subdivision. J. Environ. Manag. 87, 560–566. https://doi.org/10.1016/j.jenvman.2007.03.026

Ferreira, C.S.S., Ferreira, A.J.D., Pato, R.L., Magalhăes, M.C., Coelho, C.O., Santos, C., 2012. Rainfall-runoff-erosion relationships study for different land uses, in a sub-urban area. Z. Geomorphol. 56, 5-20. http://doi.org/10.1127/0372-8854/2012/S-00101

Ferreira, C.S.S., Walsh, R.P.D., Steenhuis, T.S., Shakesby, R.A., Nunes, J.P.N., Coelho, C.O.A., Ferreira, A.J.D., 2015. Spatiotemporal variability of hydrologic soil properties and the implications for overland flow and land management in a peri-urban mediterranean catchment. J. Hydrol. 525, 249-263. http://doi.org/10.1016/j.jhydrol.2015.03.039

Food and Agriculture Organization of the United Nations, 2007. Available online at: http://www.fao.org/geonetwork/srv/en/metadata.show?id=14116

Gentilucci, M., Barbieri, M., D'Aprile, F., Zardi, D., 2020. Analysis of extreme precipitation indices in the Marche region (central Italy), combined with the assessment of energy implications and hydrogeological risk, Energy Reports. 6, 804-810 https://doi.org/10.1016/j.egyr.2019.11.006

Giorgi, F., Lionello, P., 2008. Climate change projections for the mediterranean region. Glob. Planet. Chan. 63(2-3), 90-104. http://doi.org/10.1016/j.gloplacha.2007.09.005

Golmohammadi, G., Rudra, R., Dickinson, T., Goel, P., Veliz, M., 2017. Predicting the temporal variation of flow contributing areas using SWAT. J. Hydrol. 547, 375–386. https://doi.org/10.1016/j.jhydrol.2017.02.008

Her, Y., Frankenberger, J., Chaubey, I., Srinivasan, R., 2015. Threshold effect in HRU definition of the soil and water assessment tool. ASABE 58, 367–378. http://doi.org/10.13031/trans.58.10805

Huan, H., Jinsheng, W., Yanguo, T., 2012. Assessment and validation of groundwater vulnerability to nitrate based on a modified DRASTIC model: a case study in Jilin City of northeast China. Sci. Total Environ. 440, 14–23. http://dx.doi.org/10.1016/j.scitotenv.2012.08.037

Kazakis, N., Busico, G., Colombani, N., Mastrocicco, M., Pavlou, A., Voudouris, K., 2019. GALDIT-SUSI a modified method to account for surface water bodies in the assessment of aquifer vulnerability to seawater intrusion. J. Environ. Manag. 235, 257-265. http://doi.org/10.1016/j.jenvman.2019.01.069

Khelifa, W.B., Hermassi, T., Strohmeier, S., Zucca, C., Ziadat, F., Boufaroua, M., Habaieb, H., 2017. Parameterization of the effect of bench terraces on runoff and sediment yield by swat modeling in a small semi-arid watershed in northern Tunisia. Land Degrad. Dev. 28(5), 1568-1578. http://doi.org/10.1002/ldr.2685

Kourgialas, N.N., Karatzas, G.P., 2011. Flood management and a GIS modelling method to assess flood-hazard areas a case study. Hydrol. Sci. J. 56 (2), 212–225. https://doi.org/10.1080/02626667.2011.555836

Kumar, S., Merwade, V., 2009. Impact of Watershed Subdivision and Soil Data Resolution on SWAT Model Calibration and Parameter Uncertainty. J. Am. Water Resour. Ass. 45(5), 1179-1196. https://doi.org/10.1111/j.1752-1688.2009.00353.x

Lin, B., Chen, X., Yao, H., Chen, Y., Liu, M., Gao, L., James, A., 2015. Analyses of landuse change impacts on catchment runoff using different time indicators based on SWAT model. Ecol. Indic. 58, 55-63. https://doi.org/10.1016/j.ecolind.2015.05.031

Lin, S., Jing, C., Coles, N.A., Chaplot, V., Moore, N.J., Wu, J., 2013. Evaluating DEM source and resolution uncertainties in the Soil and Water Assessment Tool. Stoch. Environ. Res. Risk. Assess. 27, 209–221. https://doi.org/10.1007/s00477-012-0577-x

Malagò, A., Pagliero, L., Bouraoui, F., Franchini, M., 2015. Comparing calibrated parameter sets of the SWAT model for the Scandinavian and Iberian peninsulas. Hydrolog. Sci. J. 60, 949–967. http://doi.org/10.1080/02626667.2014.978332

Mastrocicco, M., Busico, G., Colombani, N., Vigliotti, M., Ruberti, D., 2019. Modelling actual and future seawater intrusion in the variconi coastal wetland (italy) due to climate and landscape changes. Water (Switzerland), 11(7). http://doi.org/10.3390/w11071502

Mattioli, A., 2012. Il Bacino del Fiume Aspio: Assetto Geostrutturale, Geomorfologia e Idrogeologia nell'analisi delle Pericolosita' Idrogeologiche. PhD diss. Polytechnic University of Marche.

Mirabella F., Barchi M.R., Lupattelli A., 2008. Seismic reflection data in the Umbria Marche Region: limits and capabilities to unravel the subsurface structure in a seismically active area. Ann. Geophys. Italy, 51, 383-396. https://doi.org/10.4401/ag-3032

Moriasi, D., Arnold, J., Van Liew, M., Bingner, R., Harmel, R., Veith, T., 2007. Model evaluation guidelines for systematic quantification of accuracy in watershed simulations. Trans. ASABE 50 (3), 885–900. http://doi.org/10.13031/2013.23153

Neitsch, S., Arnold, J., Kiniry, J., Williams, J., 2000. Soil and Water Assessment Tool Theoretical Documentation 2000. Grassland, soil and water research laboratory, Agricultural Research Service, 808 East Blackland Road, Temple, Texas 76502, 506 pp.

Pappenberger, F., Beven, K.J., Hunter, N.M., Bates, P.D., Gouweleeuw, B.T., Thielen, J., de Roo, A.P.J., 2005. Cascading model uncertainty from medium range weather forecasts (10 days) through a rainfall-runoff model to flood inundation predictions within the European Flood Forecasting System (EFFS). Hydrol. Earth Syst. Sci. 9(4), 381-393. https://doi.org/10.5194/hess-9-381-2005.

Pellegrini, M., 2019. A 19-Years Period (2000-2018) Dataset of Annual and Monthly Spatial Distribution of Rainfall and Average Air Temperature in a Temperate Region for Climate Change Studies. Asian J. Res. Rev. Phys. 2(4), 1-6. http://www.journalajr2p.com/index.php/AJR2P/article/view/30106

Rosolem, R., Gupta, H.V., Shuttleworth, W.J., Zeng, X., de Goncalves, L.G.G., 2012. A fully multiple-criteria implementation of the Sobol' method for parameter sensitivity analysis. J. Geophys. Res. 117, D07103. http://dx.doi.org/10.1029/ 2011JD016355.

Rouholahnejad, E., Abbaspour, K. C., Vejdani, M., Srinivasan, R., Schulin, R., Lehmann, A., 2012. A parallelization framework for calibration of hydrological models. Environ. Model. Softw. 31, 28-36. http://doi.org/10.1016/j.envsoft.2011.12.001.

Schüler, G., 2007. Runoff generation and forestry measures to mitigate floods. Prog. Hydro-Sci. Eng. 3, 197–211

Scussolini, P., Aerts, J.C., Jongman, B., Bouwer, L.M., Winsemius, H.C., de Moel, H., Ward, P.J., 2016. FLOPROS: an evolving global database of flood protection standards. Nat. Hazards Earth Syst. Sci, 16(5), 1049-1061. https://doi.org/10.5194/nhess-16-1049-2016.

Shadmehri Toosi, A., Calbimonte, G.H., Nouri, H., Alaghmand, S., 2019. River basin-scale flood hazard assessment using a modified multi-criteria decision analysis approach: A case study. J. Hydrol. 574, 660-671. http://doi.org/10.1016/j.jhydrol.2019.04.072.

Shen, Z., Chen, L., Chen, T., 2011. Analysis of parameter uncertainty in hydrological modeling using GLUE method: a case study of SWAT model applied to Three Gorges Reservoir Region, China. Hydrol. Earth Syst. Sci. 8, 8203–8229. https://doi.org/10.5194/hess-16-121-2012.

SIRMIP, 2020. Available online at: http://app.protezionecivile.marche.it/sol/indexjs.sol?lang=en

Sokolowski, J., Banks, C., 2011. Principles of Modeling and Simulation: a Multidisciplinary Approach. John Wiley and Sons, Hoboken, New Jersey, USA.

Song, X., Zhang, J., Zhan, C., Xuan, Y., Ye, M., Xu, C., 2015. Global sensitivity analysis in hydrological modeling: Review of concepts, methods, theoretical framework, and applications. J. Hydrol. 523, 739-757. http://doi.org/10.1016/j.jhydrol.2015.02.013

Tasdighi, A., Arabi, M., Harmel, D., 2018. A probabilistic appraisal of rainfall-runoff modeling approaches within SWAT in mixed land use watersheds. J. Hydrol. 564, 476-489. http://doi.org/10.1016/j.jhydrol.2018.07.035.

Tazioli, A., Mattioli, A., Nanni, T., Vivalda, P.M., 2015. Natural hazard analysis in the Aspio equipped basin. Engineering geology for society and territory - volume 3: River basins, reservoir sedimentation and water resources. 431-435. http://doi.org/10.1007/978-3-319-09054-2_89.

Tuo, Y., Duan, Z., Disse, M., Chiogna, G., 2016. Evaluation of precipitation input for SWAT modeling in alpine catchment: A case study in the adige river basin (italy). Sci. Tot. Environ. 573, 66-82. http://doi.org/10.1016/j.scitotenv.2016.08.034

Turco, M., von Hardenberg, J., AghaKouchak, A., Llasat, M.C., Provenzale, A., Trigo, R.M., 2017. On the key role of droughts in the dynamics of summer fires in Mediterranean Europe. Sci. Rep. 7 (1), 81. https://doi.org/10.1038/s41598-017-00116-9

USDA-SCS, 1972. National engineering handbook, Section 4, Hydrology. USDA-Soil Conservation Service: Washington, DC.

Wang, X., 2014. Advances in separating effects of climate variability and human activity on stream discharge: An overview. Adv. Water Resour. 71, 209-218. https://doi.org/10.1016/j.advwatres.2014.06.007

Williams, J.R., 1995. The EPIC model. In: Singh, V.P. (Ed.), Computer Models of Watershed Hydrology. Water Resources Publications, Highlands Ranch, CO, pp. 909–1000 (Chapter 25).

WorldClim, 2020. Available online at: https://www.worldclim.org/data/cmip6/cmip6_clim2.5m.html

Zhang, P., Liu, R., Bao, Y., Wang, J., Yu, W., Shen, Z., 2014. Uncertainty of SWAT model at different DEM resolutions in a large mountainous watershed. Water Res. 53, 132-144. https://doi.org/10.1016/j.watres.2014.01.018